Journal of Aerosol Science 142 (2020) 105523

Contents lists available at ScienceDirect

Journal of Aerosol Science

journal homepage: http://www.elsevier.com/locate/jaerosci

Impact of water droplet and humidity interaction with soluble particles on the operational performance of surface filters in gas cleaning applications

Almuth D. Schwarz *, Leonie König, Jörg Meyer, Achim Dittler

Karlsruhe Institute of Technology, Institute of Mechanical Process Engineering and Mechanics, Straße am Forum 8, D-76131, Karlsruhe, Germany

ARTICLE INFO

Keywords:
Hygroscopic salt particles
Water droplets
Humidity
Surface filter
Deliquescence and efflorescence

ABSTRACT

The behavior of salt particles on a surface filter exposed to a high humidity gas flow and water droplets was studied to gain a better understanding of the influence of water content in its different states on the operating behavior of such filters. Two sets of experiments were carried out: in both, polydisperse sodium chloride particles were filtered from a dry air stream onto hydrophobic filter media, which were subsequently exposed to either relative humidity above the deliquescence relative humidity or to water droplets. Results show that the rearrangement of salt particles on the filter face side takes place in both sets of experiments. However, rearrangements resulting from the influence of high humidity can be clearly distinguished from the ones resulting from contact with water droplets. Recordings of the pressure drop across the test filters, as well as scanning electron microscope micrographs of the sodium chloride particles on the upstream face side of the medium, show this difference clearly. No penetration of salt particles through the filter medium occurred under the conditions presented in this study.

1. Introduction

Surface filtration is an efficient and frequently used method to separate particles from dust-loaded gas streams. During this process, the filter is often exposed to a constant aerosol flow. Upon contact with the filter medium, particles from the aerosol deposit. With more particles being separated, a particle layer forms, a so-called filter cake. As the filter cake grows and its thickness increases, the filtration efficiency as well as the pressure drop across the filter increase. At a predetermined maximum pressure drop, the filter cake can be removed and a new filtration cycle starts. The operating behavior of the process is greatly determined, among other factors, by the composition of the present aerosol itself, including particle concentrations and sizes, its chemical compounds and the ambient water content in the form of liquid droplets and humidity.

In some industrial applications, for example the filtration of the inlet airstream of gas turbines, the presence of high humidity and the subsequent condensation of water onto the filter media has been connected with filtration inefficiencies and turbine failure (Wilcox, Ransom, & Delgado-Garibay, 2010). Due to the high salt and water content in the intake air, coastal, marine and off-shore applications are especially prone to these issues.

The full influence of air moisture content on filtration processes is still not fully understood and can only be described phenomenologically, as it depends on many different parameters such as the hygroscopicity of the particles, their size, their chemical

* Corresponding author.
E-mail address: almuth.schwarz@kit.edu (A.D. Schwarz).

https://doi.org/10.1016/j.jaerosci.2020.105523
Received 2 August 2019; Received in revised form 11 December 2019; Accepted 19 January 2020
Available online 22 January 2020

Table 1
Overview of presented literature and according material systems.

#	Authors	Filter material	Cake filtration	Aerosol type			Filtr. velocity	Temp.	Rel. humidity	Preloaded filter
				Hygroscopic	Non-Hygroscopic	Liquid				
	/-	/-	/-	/-	/-	/-	/cm s^{-1}	/°C	/as indicated	/-
1	Agranovski and Braddock (1998)	wettable glass fiber	no	–	–	H_2O 0.1–20 µm	100	20	85%	no
2	Boudhan et al. (2019)	bag filter PTFE	yes	–	submicronic C	–	1.9	150	0 & 73 g m^{-3}[a]	no
3	Contal et al. (2003)	fibrous depth filters	no	–	–	submicronic DOP, Glycerol, DMP	2.5	–	–	no
4	Gupta et al. (1993)	HEPA	yes	1 and 0.5 µm NaCl	1 and 0.5 µm AL_2O_3[a]	–	3	25	35 - 90%	no
5	Horst et al. (2018)	single fibers: Cu, Fe, PET, PA, PTFE	no	NaCl, KCl, K_2SO_4	–	–	NA	NA	0 - 100%	yes
6	Horst et al. (2019)	needle felts	yes	submicronic NaCl	micronic limestone	–	5	20–25	0 - 80%	yes
7	Joubert et al. (2010)	HEPA, flat and pleated	yes	submicronic NaCl	micronic Al_2O_3	–	flat media: 4–7 pleated media: 2.6	25 ±2	18 - 100%	no
8	Joubert et al. (2011)	HEPA, flat and pleated	yes	submicronic NaCl	micronic $A_{l2}O_3$	–	4–7	25 ±2	~0–~100%	yes
9	Kampa et al. (2015)	glass fiber	no	–	–	mineral oils	30	–	–	no
10	König et al. (2018)	glass fiber and membrane	yes	NaCl	–	H_2O, DEHS	2, 8, 20	–	30 - 90%	yes
12	Miguel (2003)	polyester fiber	no	0.5 and 1.3 µm NaCl	Al_2O_3 (0.8, 1.4, 6 µm)	–	2.5, 15	25 ±4	32 - 90%	no
13	Montgomery, Green, and Rogak (2015)	HVAC: electret and mechanical	no	100 nm NaCl	400 nm AlO_3	–	11	–	0 - 60%	yes
14	Pei et al. (2019)	cellulose fiber	no	submicronic KCl, $(NH4)_2SO_4$, NH_4NO_2	–	–	5.3	–	15–75%	no
15	Ribeyre, Charvet, Valliéres, and Thomas (2017)	sintered plate	yes	–	nanosized Zn–Al, C, hydrophilicSiO_2	–	2.55, cake filtration: 14.4	–	0 - 85%	yes
16	Schmidt, Breisenbacher, and Suhartiningsih (2013)	glass fiber	yes	NaCl	Arizona test dust (A2)	H_2O	15	23	30 - 90%	yes
17	Zhang (2017)	polyester needle felt	yes	0.35 µm NaCl	limestone (3.1 µm)	–	–	–	< and > DRH	yes
18	Schwarz et al. (paper at hand)	glass fiber	beginning of cake filtration	submicronic NaCl	–	H_2O	3.5	25	<10–100%	yes

[a] Absolute humidity (T > 100 °C at ambient pressure).

composition, the degree of water content and the design of the filter. Agranovski and Braddock (1998) investigate the separation efficiency of water aerosol on hydrophilic and hydrophobic filters and find that the flow channels of water and air in the medium strongly depend on the filter's wettability. Additionally, Contal et al. (2003) relate the redistribution of liquid collected on fibrous filters to the filter properties, especially fiber diameter, packing density and pore size distribution. Compared to the field of liquid filtration, the effect of humidity on aerosol filtration processes is less frequently discussed in literature. The majority of literature deals with the effects of humidity on inert, insoluble particles. Ribeyre, Charvet, Vallieres and Thomas (2017) for example, report a decrease in filter cake thickness and a resulting pressure drop increase for nanosized non-hygroscopic filter cakes with rising humidity. They assume this phenomenon to be the result of modified internal forces of the nanostructured deposit due to liquid bridges between particles at relative humidity above 70%.

Further studies have been conducted with hygroscopic and soluble particles, most of which focus on operating conditions below the deliquescence relative humidity (DRH). The DRH describes the specific humidity for a compound, at which it dissolves by absorbing water from the surrounding atmosphere. The reverse effect, efflorescence, takes place when the solution is dried, and a crystal is formed. The efflorescence relative humidity (ERH) does not equal the DRH. The resulting structure of hygroscopic particles after undergoing efflorescence greatly depends on the substance itself, the time during which the drying takes place and the morphology of the surface, which the particles are in contact with. Horst, Zhang, and Schmidt (2018) observe the deliquescence and efflorescence process of sodium chloride particles on single fibers with an environmental scanning electron microscope. After undergoing efflorescence on hydrophobic surfaces, the salts used in the study showed their characteristic cubic crystal shape, whereas on hydrophilic copper fibers recrystallization lead to a crust formation of the salt on the fibers. Pei, Ou, and Pui (2019) found that for individual salt particles on a cellulose filter media with elevated humidity even below DRH during filtration, water is being absorbed by the salt and the particle size increases.

In filtration processes, Gupta, Novick, Biswas, and Monson (1993) report a linear pressure drop increase across HEPA filters during the filtration of hygroscopic sodium chloride particles with mass median diameters of 0.5 μm and 1 μm exposed to humidity below their DRH and a steep non-linear increase in pressure drop with collected mass per filtration area at humidities above their DRH during the filtration. They assume the increasing pressure drop was caused by the penetration of liquid into the filter media where it formed a film, but they were unable to verify this assumption. Joubert, Laborde, Bouilloux, Callé-Chazelet, and Thomas (2010) investigate the effect of relative humidity on the filtration behavior of hygroscopic, submicronic sodium chloride and non-hygroscopic, micronic aluminium oxide particles on HEPA filters. In accordance with the results by Gupta et al. it was found that for the filtration with non-hygroscopic and with hygroscopic aerosols below the DRH, the pressure drop over the filter increases linearly. Above the deliquescence point, the observed pressure drop increases with a "jump", which is characteristic for liquid filtration as described in the jump-and-channel model by Kampa, Wurster, Meyer, and Kasper (2015), which was originally developed for oil mist filters. The obtained results allowed Joubert et al. to set up a semi-empirical model investigating the pressure drop across filters during the filtration of non-hygroscopic particles in the presence of humidity and, with hygroscopic particles, in the presence of humidity, below their DRH (Joubert, Laborde, Bouilloux, Callé-Chazelet, & Thomas, 2011). Other authors conducting experiments with different materials made similar observations concerning the operating behavior. Miguel (2003) presents comparable findings with sodium chloride particles at elevated humidity during the filtration with filters made of polyester fiber. Montgomery, Sheldon, Green and Rogak (2015) investigate sodium chloride and submicronic aluminum oxide on electret and mechanical HVAC filters at up to 60% relative humidity and draw similar conclusions. Also Schmidt, Breidenbach and Suhartininghsih (2013) report a pressure drop decrease for compact glass fiber filters with initially dry sodium chloride particles after the exposure to elevated humidity below the DRH and a pressure drop increase above the DRH. Boudhan, Joubert, Durécu, Gueraoui, and Le Coq (2019) conduct studies with pulse-jet bag filters at temperatures of 150 °C with varying absolute humidity. A faster increase in the pressure drop was recorded during the filtration of a non-hygroscopic carbon aerosol at high absolute humidity, which was explained by water capillary condensation.

Zhang (2017) points out the potential of raw gas conditioning using hygroscopic particles during surface filtration. In their most recent study Horst, Zhang, and Schmidt (2019) show the effect of humidity above the DRH on filter cakes formed from non-hygroscopic limestone particles with added fractions of submicronic sodium chloride particles. They found that deliquescence and efflorescence of hygroscopic salt particles in dust cakes can have a significant impact on the operating behavior and regeneration of surface filters and have the potential to improve the cake removal.

The effects of water droplets on soluble filter cakes were investigated by König, Schmidt, and Engelke (2018). They exposed sodium chloride filter cakes formed on membranes and glass fiber filter media to varying humidity or water droplets. The findings included that the filtration efficiency can increase or decrease due to the contact with water droplets depending on the material of the filter media. In all cases, the effects were more pronounced after exposure to water droplets compared to high humidity only. Unfortunately, explanations or further details about the filter material were not provided.

Table 1 provides an overview of the literature cited in this short introduction including respective material systems and relevant operating conditions.

Overall, the main motivation for previous investigations was to examine the effects of varying water content, mainly humidity, on the filtration efficiency rather than the mechanisms taking place, and consequently the effect on the particles present in the system. In this work, we investigate the possible influences soluble particles could have on filtration processes in the presence of high humidity, above the DRH, and liquid droplets. To our knowledge, the shifting and penetration of solubles with the direction of flow into the medium or even through it due to the presence of solvent have not been part of any previous publications. The authors assume two main penetration effects, which liquid droplets could have on a soluble filter cake as schematically illustrated in Fig. 1: penetration into the filter medium and structural rearrangement after drying, or full penetration of the solution through the medium. Both effects

presume movement of the solution with the direction of the gas flow. It can also move along the filter fibers perpendicular to the direction of gas flow, which can result in rearrangements of the salt particles on the upstream filter surface. As an initial step to challenge this assumption, the rearrangement of particles on the face side of the filters and the influence on the operational performance is being studied. The aim is to investigate the fundamental effects that water droplets can have on the filter cake consisting of soluble particles during a filtration process, leading to a clearer understanding of the mechanisms that take place in the system.

2. Material and methods

2.1. Aerosol and test filter

Sodium chloride served as the test salt in all experiments. It is a naturally occurring salt with a solubility of 358 g l^{-1} in water at 20 °C and atmospheric pressure. At 25 °C and atmospheric pressure, its DRH is 75.4% and its ERH is 48% (Zhang, 2017). Both, its solubility and DRH remain relatively constant with changing temperature compared to other salts. An aerosol was generated by atomizing a 10 g l^{-1} salt solution and subsequent drying with silica gel in a diffusion dryer. The particle size distribution of the dry salt particles was determined with a SMPS (TSI, Model 3082) as shown in Fig. 2. To analyze the structure of the generated salt particles and later on the formation of particles on the filter surface, images were obtained with a scanning electron microscope (SEM). Under the given conditions, the generated particles take a polyhedron shape, whose contour is better approximated with that of a sphere, rather than its characteristic cubic shape (Fig. 2). This particle shape is the reproducible result of the crystallization kinetics under the given conditions and the sudden efflorescence in the diffusion dryer.

Deionized water was used throughout the experiments for the preparation of the salt solutions, increasing the relative humidity employing a bubbler and generating water droplets utilizing an atomizer. Dry (6% rel. humidity), particle free air was used in the bubbler and atomizer, as well as for drying and conditioning the filters.

The implemented surface filters are made of hydrophobic, oleophobic polyester flat sheet media with a weight of 440 g m^{-2} and a thickness of 1.4 mm. They are circular with an active filtration area measuring 42.1 mm in diameter. The media has a permeability between 100 and 170 l dm^{-2} min^{-2} at 200 Pa. Initial pressure drops during the presented experiments vary between 20 and 40 Pa. Fig. 3 shows a photograph and a SEM image of the upstream face side of the test filter.

2.2. Experimental set-up and procedure

To decide on the degree of surface filtration being investigated in this work (e.g. established filter cake or initial phase of particle bridge formation), preliminary experiments served to gain a better understanding of the filter cake formation on the filter medium at hand. The filter was exposed to sodium chloride aerosol over a period of 4 h. Filtration velocity and particle size distributions were the same in these preliminary experiments as in all following test series. The relative humidity remained below 10% during the filtration. The pressure drop recorded over the filter and the according degrees of cake formation on SEM images at t = 60 min and at t = 180 min are shown in Fig. 4. After 3 h of exposure to salt aerosol at t = 180 min the pressure drop increases by about 17 mbar and the SEM image clearly shows a full cake formation of salt particles leaving no filter fibers visible. Letting only 60 min pass, the slope of the pressure drop has not yet reached a constant incline, which indicates that the experiments at t = 60 min were in the transition zone between depth filtration and full surface filtration. This particle formation without a full cake formation allows us to see the particle shapes not only on the outermost surface, but also inside the first layer of the filter as the SEM images show (Fig. 4). This helps to understand the influence high humidity or an increased number of water droplets could have on the filtration process at an early stage. Therefore, we decided to choose a filtration time for salt aerosol of 60 min for this study. After 60 min filtration time, a soluble particle load of 8 g m^{-2} on the filter was gravimetrically determined, which, under the given conditions, results in a salt concentration of 0.063 g m^{-3} in the raw gas.

To investigate the influence of water droplets and humidity on the soluble particles present on a surface filter, a new experimental setup was developed, which allows for the following four-step procedure (Table 2, Fig. 5):

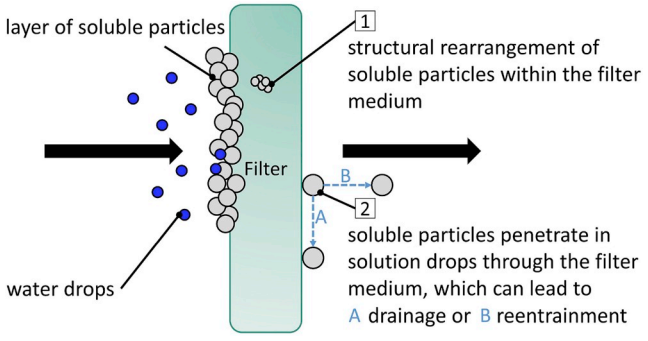

Fig. 1. Schematic illustration of possible penetration mechanisms of soluble particles exposed to liquid droplets in surface filtration processes including [1] structural rearrangement within the filter and [2] penetration to the downstream side of the filter.

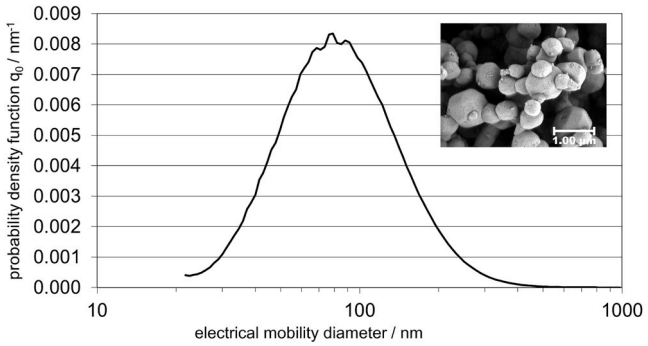

Fig. 2. Particle size distribution determined using a SMPS and an according SEM image of the sodium chloride particles.

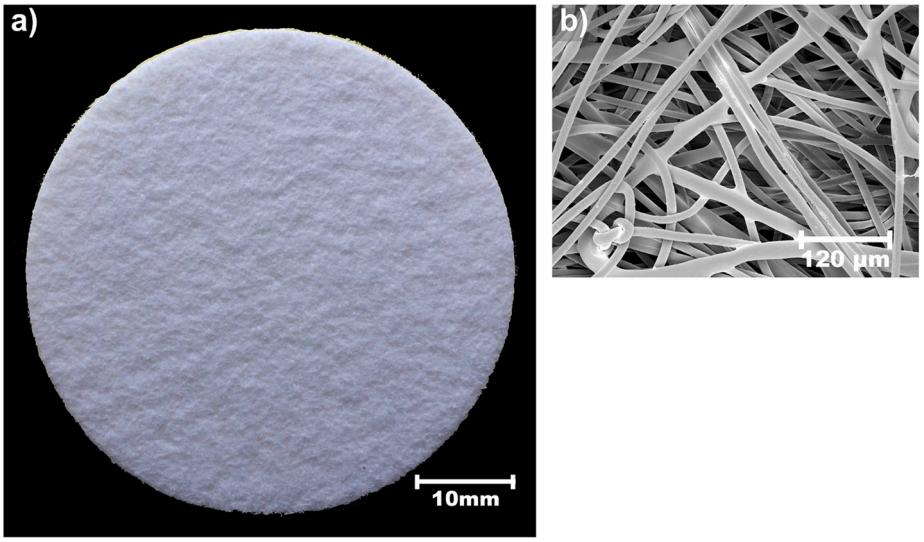

Fig. 3. Images of the face side of the filter medium used in this study as (a) a full scale photograph and (b) a SEM image.

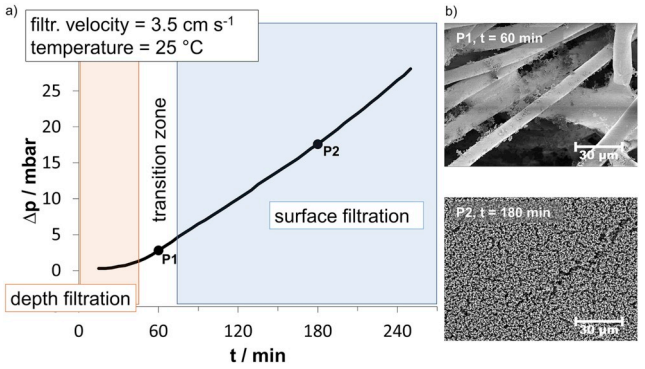

Fig. 4. The initial states of particle layer formation during surface filtration shown by a) the recorded total pressure drop across the test filter during the loading with sodium chloride particles and b) according SEM images at P1, t = 60 min and P2, t = 180 min.

During each step, a constant filter face velocity of 3.5 cm s^{-1} was maintained at a temperature of 25 °C and atmospheric pressure. The flow velocity was regularly monitored using a bubble flow meter with a precision of ±0.03 l min^{-1}.

All filters were exposed to salt aerosol for 60 min at a relative humidity below 10%. Following the loading step, the filters were conditioned with dry air for a duration of 20 min until the pressure drop remained constant, to ensure the stability of the particles on the media. Only after the conditioning of the whole system, the filters were exposed to an increased water content for 25 min. Two sets

Table 2
Procedure of the experiments including the duration of each step.

#	Procedure	Duration
1	Filtration of salt particles onto the filter	60 min
2	Conditioning of the filter with dry, particle free air	20 min
3A	Moistening of the filter with increased humidity	25 min
3B	Moistening of the filter with water droplets	25 min
4	Drying of the filter	30 min

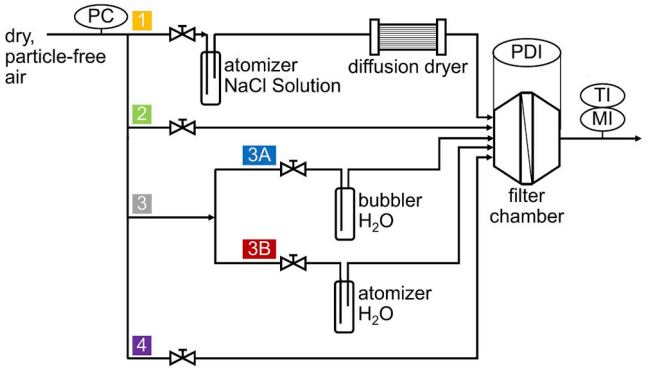

Fig. 5. Schematic setup used for the presented experiments. The numbers indicate different flow paths for the four stages of the experimental procedure with (1) filtration of salt particles onto the filter, (2) conditioning of the filter with dry air, (3) moistening of the filter cake and the filter with (3A) increased humidity or (3B) water droplets and (4) drying of the filter.

of experiments were carried out. In half of the experiments, the humidity was increased above the DRH using a bubbler. In the other half of the experiments, filters were exposed to an aerosol, which contained water droplets generated with an atomizer (Topas) with a mass flow rate of 58.4 mg min^{-1}. In the fourth and final step, the filters were dried with a dry air stream, until the relative humidity measured downstream of the filter medium reached close to 5%.

The pressure drop across the filter was recorded with a precision of ± 0.5% of measured value using connectors with identical cross-sections at a distance of 11 cm up- and downstream of the filter. The temperature ± 1 °C and relative humidity (at 25 °C ± 3% between 10 and 90%, ± 5% at all others) were recorded 40 cm downstream of the filter chamber. SEM images were taken of the face side of various filters at multiple stages during the filtration process. For both SEM and gravimetrical analysis, some of the samples had to be removed from the filter chamber after the individual procedure steps. These samples were not taken back to undergo the remaining experimental steps. Therefore, when comparing two SEM micrographs at different steps of the experiments, the pictures were not taken of the same filter. Instead, multiple samples were generated to ensure representative results and comparability.

3. Results and discussion

3.1. Pressure drop across the filters

Fig. 6 shows the recorded pressure drop and humidity for both sets of experiments, (exposure to either water droplets or high

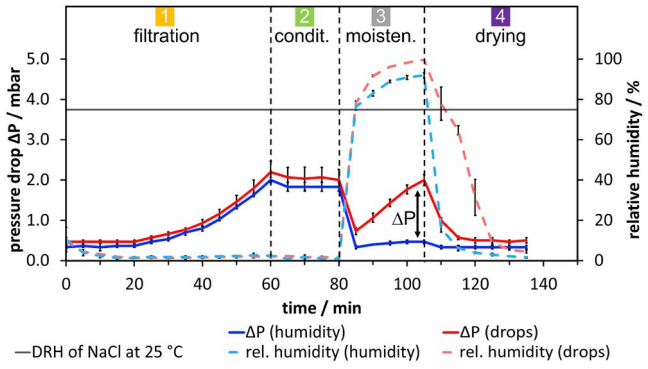

Fig. 6. Pressure drop and humidity during the experiments with the filters being exposed to high humidity (humidity) or water droplets (drops).

humidity only). The data is divided into four sections in accordance with the four procedure steps of (1) salt filtration, (2) conditioning, (3) moistening and (4) drying as described in section 2.2. The pressure drops across the filters during the first step of the filtration of salt particles increase in a similar manner in all sets of experiments as expected. Small differences in the pressure drops can be explained by the inhomogeneity of the filter material, leading to a different initial pressure drop at the very beginning of the experiment. The humidity in this first step remained below 10%. The initial decrease in humidity is the result of the initially unconditioned air inside the system due to exposure to the ambient atmosphere during the mounting of the filter sample, which is being replaced by the dry aerosol within the first 10 min of the experiments. In the 20 min of conditioning following the filtration step, the pressure drop remains constant, indicating that no structural changes take place during this phase.

In the third phase of the procedure, half of the experiments were exposed to water droplets and the other half to a humidity above the DRH of sodium chloride at 75.4%, as indicated in Fig. 6. Within the first 5 min of introducing water content into the system, the humidity reaches a value above that of the DRH. During this time, the pressure drops for both sets of experiments already show a strong decrease. Only after that, at even higher humidity, the two systems show different behaviors. Whereas the pressure drop at high humidity without direct exposure to droplets, remains almost constant following the initial decrease, the introduction of water droplets into the system leads to a steep rise in the pressure drop. The two curves converge again during the drying of the filter. The humidity recordings during this fourth step show that the humidity during the experimental runs with filters exposed to water decreases slower, as the filters take longer time to dry.

The error bars in Fig. 6 indicate that the results are reproducible. Only during rapid changes in the relative humidity, increased fluctuations can be observed, which is not surprising as small changes in filter media, salt- or water content in the system can lead to slightly different drying rates.

The difference in the pressure drops between phase two and four of the experiments is a clear sign of the rearrangement of the soluble particles on the filters between those two steps during phase three. The initial decrease of the pressure drop during phase three is an indication of the salt particles dissolving at the elevated humidity. High humidity only and the direct exposure to water droplets result in different filtration behaviors. During the exposure to liquid droplets, the total liquid content in the system is larger. As liquid droplets continue being collected on the fiber the pressure drop increases. Similarly to Gupta et al. (1993), the spreading of liquid on the filter surface is assumed to be the reason for the increase in pressure drop for the filters, which came in contact with water droplets. A visual observation of this was not possible at this stage. When first exposed to liquid droplets or high humidity, the hygroscopic salt particles soak up the water, mobilize and dissolve. The solution distributes on the hydrophobic filter surface resulting in a pressure drop increase, which is especially steep when water aerosol is present. An additional indication of water accumulation on the filters exposed to droplets is the slower decrease of humidity in the final drying step of the experiments.

3.2. Scanning electron microscope images of filters

Fig. 7 shows SEM images of the face side of the filter unloaded (Fig. 7a) and with sodium chloride particles deposited on the fibers (Fig. 7b). The picture shown in Fig. 7b was taken of a sample, which was removed from the experiments after the initial step of filtering salt particles from a stream of dry air. As previously discussed (Section 2.1), no full filter cake has been formed at this stage. The particles show an almost round shape and are attached either to the fiber itself or other particles, as expected during the initial phase of filter cake formation. Next to single particles, dendritic agglomerated structures are visible.

Further micrographs were recorded with the SEM of the filters after undergoing all four steps of the experiments, including the exposure to high humidity and water droplets and the subsequent drying. After introducing a humidity above the DRH and liquid water, the SEM images show a relocation of particles on the filters.

Fig. 8 shows SEM images of dried salt deposited on a filter after the exposure to high humidity (Fig. 8a) and after exposure to high humidity and liquid droplets (Fig. 8b).

Fig. 8a shows that fewer, bigger particles with the characteristic cubic crystal shape of sodium chloride remain on the face side of the filter compared to the initial particle structures shown in Fig. 7b. The difference in the crystal shape between the crystals after the exposure to dry salt aerosol and those after the exposure to humidity above the DRH can be explained by the differences in the drying process of the salt in those two cases. In the initial phase of the experiment, the particles were dried in the gas stream in a diffusion dryer with a calculated mean residence time of less than 15 s. The drying process at the end of each experiment lasts multiple minutes, as shown in Fig. 6. Additionally, surface interactions influence the crystal shape. The particles show their specific crystal shapes on the hydrophobic surface as expected when comparing the results to the findings of Horst et al. (2019).

After exposure to water droplets, even fewer particles can be found on the face side of the filter compared to the filters exposed to high humidity only (Fig. 8b), but the drying process also left them in their characteristic cubic shape at the end of the experiment.

During the experiments, no penetration of water through the medium was visible on the clean gas side of the filter and no particles were detected by an SMPS after drying the clean gas stream with a diffusion dryer. Therefore, it can be expected that no penetration of salt particles through the filter occurred during the experiments.

The SEM images of the filters exposed to water droplets show, that salt has disappeared from the face side of the filter. As no penetration through the filter medium was detected, it must be assumed that the salt penetrated into the medium where it subsequently dried. Unfortunately, SEM images of the cross section of the filters did not lead to conclusive results, but will be subject to further investigations. It remains unclear where exactly and in which shape the salt particles dried at the end of this set of experiments.

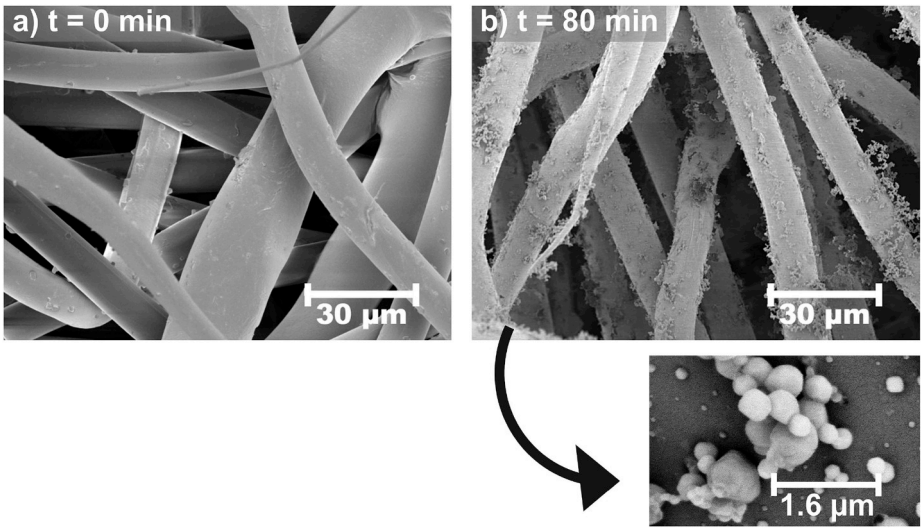

Fig. 7. SEM image of the (a) clean face side of the filter at t = 0 min and (b) face side of the filter after the filtration and conditioning of dry salt aerosol at t = 80 min.

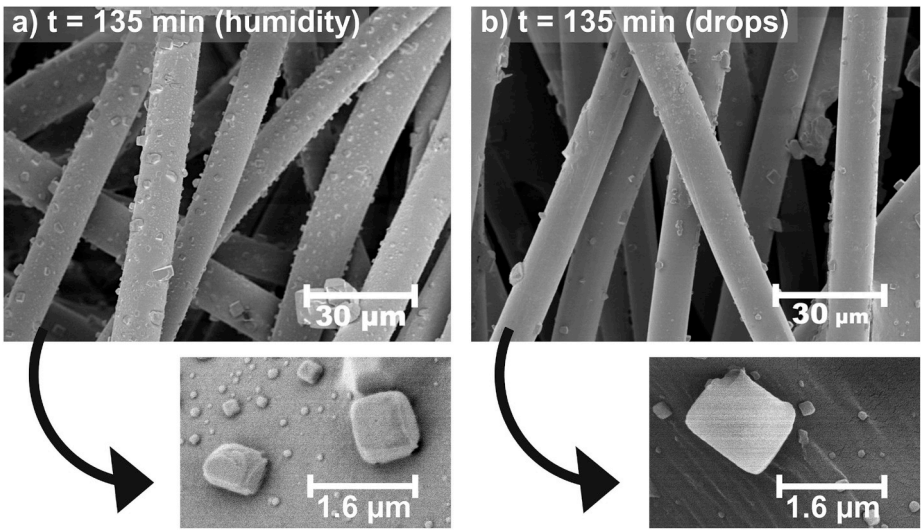

Fig. 8. SEM image of (a) salt particles on the face side of the filter after exposure to humidity and subsequent drying at t = 135 min and (b) salt particles on the face side of the filter after exposure to water droplets and subsequent drying at t = 135 min.

4. Conclusion

In two sets of experiments, this study investigates the initial effects of humidity above the DRH and water droplets on a soluble particulate deposit on a surface filter. Sodium chloride was separated from a dry aerosol stream onto a surface filter. Subsequently, it was exposed to either a humidity above the DRH of sodium chloride, or to water droplets.

The results showed that the exposure of soluble particles on a hydrophobic surface filter to both, high humidity only and to water droplets results in rearrangements of the particles on the face side of the filter. Using pressure drop recordings and SEM images taken after the experiments the two sets of experiments can be clearly distinguished. The pressure drop showed a steeper increase for a loaded filter exposed to water droplets compared to high humidity only, which is likely the result of accumulated liquid on the face side of the hydrophobic filter.

The salt on the filter surfaces takes its characteristic cubic shape on the hydrophobic filter after being exposed to humidity above the DRH. Further experiments with hydrophilic mediums have to be conducted to compare resulting particle shapes and to investigate the relevance of the markup of the filter in the initial phase of filter cake formation.

The experiments showed that fewer particles remained on the face side of the filter after it is exposed to water droplets, compared

with high humidity only. As no full penetration of water or salt was detected, it has yet to be determined how far the salt particles penetrated into the medium after direct contact with water droplets. A detailed investigation will be part of further research in this field.

Acknowledgement

We gratefully acknowledge that this project was funded by the Deutsche Forschungsgemeinschaft (DFG, German Research Foundation) – 406085079.

References

Agranovski, I. E., & Braddock, R. D. (1998). Filtration of liquid aerosols on nonwettable fibrous filters. *American Institute of Chemical Engineers Journal, 44*(12), 2784–2790. https://doi.org/10.1002/aic.690441218.

Boudhan, R., Joubert, A., Durécu, S., Gueraoui, K., & Le Coq, L. (2019). Influence of air humidity on particle filtration performance of a pulse-jet bag filter. *Journal of Aerosol Science, 130*, 1–9. https://doi.org/10.1016/j.jaerosci.2019.01.002.

Contal, A., Simao, J., Thomas, D., Frising, T., Callé, S., Appert-Collin, J. C., et al. (2003). Clogging of fibre filters by submicron droplets. Phenomena and influence of operating conditions. *Journal of Aerosol Science, 35*, 263–278. https://doi.org/10.1016/j.jaerosci.2003.07.003.

Gupta, A., Novick, V. J., Biswas, P., & Monson, P. R. (1993). Effect of humidity and particle hygroscopicity on the mass loading capacity of high efficiency particulate air (HEPA) filters. *Aerosol Science and Technology, 19*(1), 94–107. https://doi.org/10.1080/02786829308959624.

Horst, D., Zhang, Q., & Schmidt, E. (2018). Deliqueszenz und Effloreszenz hygroskopischer Salzpartikeln in Partikel-Wand- und Partikel-Partikel-Kontakten. *Chemie Ingenieur Technik, 91*(1–2), 46–54. https://doi.org/10.1002/cite.201800063.

Horst, D., Zhang, Q., & Schmidt, E. (2019). Deliquescence and efflorescence of hygroscopic salt particles in dust cakes on surface filters. *Chemical Engineering & Technology, 42*(11), 2348–2357. https://doi.org/10.1002/ceat.201800754.

Joubert, A., Laborde, J. C., Bouilloux, L., Callé-Chazelet, S., & Thomas, D. (2010). Influence of humidity on clogging of flat and pleated HEPA filters. *Aerosol Science and Technology, 44*, 1065–1076. https://doi.org/10.1080/02786826.2010.510154.

Joubert, A., Laborde, J. C., Bouilloux, L., Callé-Chazelet, S., & Thomas, D. (2011). Modelling the pressure drop across HEPA filters during cake filtration in the presence of humidity. *Chemical Engineering Journal, 166*(2), 616–623. https://doi.org/10.1016/j.cej.2010.11.033.

Kampa, D., Wurster, S., Meyer, J., & Kasper, G. (2015). Validation of a new phenomenological „jump-and-channel“ model for the wet pressure drop of oil mist filters. *Chemical Engineering Science, 122*, 150–160. https://doi.org/10.1016/j.ces.2014.09.021.

König, C., Schmidt, F., & Engelke, T. (2018). Efficiency of air filters at high relative humidity or exposed to water droplets. *Chemie Ingenieur Technik, 90*(7), 1005–1010. https://doi.org/10.1002/cite.201700012.

Miguel, A. F. (2003). Effect of air humidity on the evolution of permeability and performance of a fibrous filter during loading with hygroscopic and non-hygroscopic particles. *Journal of Aerosol Science, 34*(Issue 6), 783–799. https://doi.org/10.1016/S0021-8502(03)00027-2.

Montgomery, J. F., Green, S. I., & Rogak, S. N. (2015). Impact of relative humidity on HVAC filters loaded with hygroscopic and non-hygroscopic particles. *Aerosol Science and Technology, 49*, 322–331. https://doi.org/10.1080/02786826.2015.1026433.

Pei, C., Ou, Q., & Pui, D. Y. H. (2019). Effect of relative humidity on loading characteristics of cellulose filter media by submicrometer potassium chloride, ammonium sulfate, and ammonium nitrate particles. *Separation and Purification Technology, 212*, 75–83. https://doi.org/10.1016/j.seppur.2018.11.009.

Ribeyre, Q., Charvet, A., Valliéres, C., & Thomas, D. (2017). Impact of relative humidity on a nanostructured filter cake – experimental and modelling approaches. *Chemical Engineering Science, 161*, 109–116. https://doi.org/10.1016/j.ces.2016.12.013.

Schmidt, F., Breisenbacher, A., & Suhartiningsih, S. (2013). Der Druckverlust von Luftfiltern bei hohen relativen Feuchten und bei Beaufschlagung mit Wassertröpfchen. *F&S Filtrieren und separieren, 27*, 1.

Wilcox, M., Ransom, D., & Delgado-Garibay, H. (2010, June). Filter failure during high humidity conditions. In *Conference paper at the ASME turbo expo 2010: Power for land, sea, and air* (Glasgow, UK).

Zhang, Q. (2017). Influence of an added fraction of hygroscopic salt particles on the operating behavior of surface filters for dust separation. *Chemical Engineering & Technology, 41*, 90–95. https://doi.org/10.1002/ceat.201700112.